New transmission line model of an insulated cable embedded in gel for MRI radiofrequency interaction hazard evaluation as an alternative to the transfer function model

Alexia Missoffe

New transmission line model of an insulated cable embedded in gel for MRI radiofrequency interaction hazard evaluation as an alternative to the transfer function model.

Alexia Missoffe[1]

[1]IADI, U947, INSERM, Université de Lorraine, Nancy, France

Corresponding author : Alexia Missoffe, IADI (Université de Lorraine-INSERM), Bâtiment Recherche (anciennement EFS), Rez-de-Chaussé, CHRU de Nancy Brabois, Rue du Morvan, FR-54511 Vandoeuvre Cedex. Tel : 0033383157481. email : alexia.missoffe@univ-lorraine.fr

Abstract: 196 words
Text: 5181 words
Number of figures: 5
Number of tables : 3
Number of references : 15

Keywords: radiofrequency, transmission line, transfer function, MRI safety, pacemaker

Acknowledgement: The author thanks Julie Kabil, my aunt Colette Thomson for correcting the English. And finally Cédric Pasquier for the funding through Region Lorraine and FEDER.

ABSTRACT

Object: To demonstrate the possibility to model the power deposited at the electrode of an insulated cable in gel at 64MHz with a transmission line model with a strictly passive electrode model. This offers a more related to physics alternative to the transfer function model. The equivalence between both models is shown.

Materials and Methods: In a first step, the possibility of modeling an insulated cable with a transmission line model was analyzed through full-wave numerical simulations. An electrode model that has a physical meaning was proposed. The transmission line model predictions were confronted to experimental and simulated data of the transfer function of a cable and of the resonant behavior as a function of length of cables with different termination conditions.

Results: The assumption of a transmission line model which underlies the transfer function model is right for a simple cable embedded in tissue imitating gel. A transmission line model extracted from a transfer function allows to predict the resonant behavior of two cables with different termination conditions.

Conclusion: A transmission line model of an insulated cable embedded in tissue imitating gel offers a more directly related to physics alternative to the transfer function model.

Keywords: radiofrequency, transmission line, transfer function, MRI safety, heating, pacemaker

INTRODUCTION

Magnetic Resonance Imaging is an essential imaging modality for soft tissue imaging. Nevertheless, it presents a risk for patients implanted with a medical device. In particular, there is a risk concerning the radiofrequency field for active implants with long leads such as neurostimulators, pacemakers or defibrillators. Indeed, the induced currents along the lead can lead to heating of the tissues around the bare electrode at the end of the lead and induced voltages at the input impedance of the active device. Simulation plays an important role in the study of lead interactions with the radiofrequency field as it facilitates the collection of important information without the cost of MRI time. Currently the leads of the implanted devices mentioned are generally too complex to be simulated by the numerical resolution of full-wave Maxwell equations [1]. The problematic of simulating coaxial helicoidal pacemaker leads has been studied by Talcoth *et al.* [1] leading to the conclusion that the approximations necessary to allow pacemaker lead simulation are too coarse. Indeed because of the consequence of the proximity effect on current for two adjacent windings, the full 3D geometry of the winded wires has to be taken into account which would lead to unacceptable simulation times. An alternative to the full-wave simulation is to use the transfer function model proposed by Park *et al.* [2] that can be evaluated experimentally. This model, once determined, allows to evaluate in a very straight forward manner the heating at the electrode for any distribution of the incident field along the path of the lead. Especially, one can run a full-wave simulation of anatomical models without the lead to extract the possible incident field along the path of a device lead. The transfer function model then allows the evaluation of the heating risk in an anatomical environment. The transfer function model is all the more important so as the phase distribution of the incident field in a human body model has a crucial importance on the heating effect at the electrode. These so called “phase effects” were brought to light by Yeung *et al.* [3] in 2002 and this work was at the origin of

the transfer function concept proposed later [2]. The realistic phase distribution of the incident field in a human body is usually not experimentally reproducible in phantoms with standard radiofrequency MRI coils. Therefore it is essential to have a theoretical model to link the heating at the electrode to the real incident field distribution.

In the article by Yeung et al.[3], the fact that the heating at the electrode depends linearly on only the incident electrical field along the path of the cable comes directly from the formulation of the numerical resolution of the problem by the method of moments. Park et al. [2] suggested that the work by King [4] on transmission line models of antennas embedded in matter could be useful to determine the transfer function of a simple cable for which analytical expression of the parameters exist. Also, according to Feng et al. [5] the underlying assumption under the transfer function model is that a transmission line model is valid to describe the behavior of the cable embedded in gel at the frequency of interest.

The work of King [6] inspired the modified transmission line model proposed by Acikel *et al.*[7]. This model considers the ambient conducting medium to be the return path for the current. The main adjustment made from the model by King et al. was to integrate the fact that the excitation was no more a point excitation at the end of the insulated cable but a field distribution all along the cable generated by another antenna. They evaluate the transmission line parameters for bare and insulated wires using a theoretical analytical analysis and show that their model correctly predicts the full-wave simulation current distribution along different wires. In this work [7], for the insulated wire, the current distributions fall progressively to zero at the ends suggesting that they are also isolated at the end, the end loads being considered as infinite.

An issue of this transmission line model is actually to correctly model the bare electrode at the end of the insulated cable which corresponds neither to a short-circuit nor to an open circuit. In [4], King considers that the impedance of a bare portion of the cable at the end of an insulated cable can be calculated from the expression of the impedance of a bare monopole in a homogeneous media determined in previous work [8]. Alternatively Acikel *et al.*[9] propose an electrode model which is a voltage source associated to an impedance. The voltage source models the incident field influence and is normalized to it. Nevertheless, it seems non physical to have to model a completely passive element such as an electrode embedded in gel by a voltage source as if it acted as an incident field amplifier. In the work presented here, we present a transmission line model with an electrode model which is a simple complex load impedance meaning a strictly passive element as suggested by King [4]. This model has a physical meaning and might even be a measurable parameter in the future.

An issue that also appears here is the definition of the voltage along the transmission line. Here the second conductor, which is the return path for the current, is made of the slightly conducting ambient medium. At the surface of the insulation, the electrical field decays exponentially in the gel with a characteristic distance which is not negligible therefore necessitating a new definition of the voltage drop between the two conductors. Acikel et al.[10] explain that the voltage is a scaled version of the charge distribution at the surface of the insulated cable. It seems nevertheless necessary to give a physical definition of the transmission line voltage that can be quantitatively calculated from the field distributions. This work proposes a definition. The proposed definition of the voltage along the line allows the simple extraction of the load impedance from a full-wave simulation.

To sum up, this work presents a model based on the modified transmission line method (MoTLim) presented by Acikel *et al.*[7] inspired from earlier work by King [6] but with a strictly passive model for the end electrodes. It specifically focuses on showing that this model is indeed an alternative to the transfer function model having the advantage of being described by a set of more physical parameters than the mathematical transfer function model.

We concentrated on a wire similar to the standard S-AIMD 1 wire from the ISO-TS 10974 norm [11] for active implants and we varied the length and termination conditions. We first studied the data extracted from full-wave simulations at 64 MHz (1.5T MRI), to evaluate if indeed an insulated wire embedded in gel can be described by the modified transmission line theory meaning that the incident field, voltage and current distribution along the cable respect the modified transmission line equations. A second part focused on the equivalence with the transfer function model and how the transmission line model can predict experimental and simulated transfer functions. A third part shows the transmission line model can predict the experimental and full-wave simulated resonant behavior of the heating at the electrode as a function of length of two different cables with two different distal electrode termination conditions.

MATERIAL AND METHODS

Determination of a transmission line model from a full-wave numerical simulation

The wire studied was a steel wire with a 1.5 mm diameter isolated by a 0.5 mm thick heat-shrinkable tube made of polyolefin. Steel was considered to be a perfect electrical conductor at the working frequency of 64 MHz. The measured insulation permittivity at 64MHz was 2.35+/-0.01. The wire studied to extract the transmission line parameters was a 20 cm wire of the type described above with 1 cm of insulation removed at both ends.

The full-wave simulations were performed using the software SEMCAD-X v14.8 (SPEAG, Zurich, Switzerland). The cable was placed in an American Society for Testing and Materials (ASTM) [12] phantom filled with gel with a relative permittivity ε_r of 80 and a conductivity of 0.47 S/m. The excitation used was a plane wave excitation in a volume of 208 x 110 x 640 mm encompassing the cable. The boundary conditions were set up such as to imitate an infinite volume of the ASTM gel. The cable was placed along the z-axis of the phantom. The plane-wave excitation had a propagation direction along the direction x, the electrical field direction being along z meaning it was parallel to the cable direction which is necessary to induce currents therefore heating at the bare electrodes. The simulation was a 20 period harmonic simulation at 64 MHz. A simulation without the cable was performed to extract the incident field along the cable which is the entry to the transmission line model. We worked in the frequency domain, all variables were phasors which are the complex representative of the sinusoidally time varying fields characterized by an amplitude and a phase.

The power deposited at the electrode was considered to be proportional to the active power at the load impedance modeling it. The actual output wanted from the model is the voltage or the current at the load impedance. Nevertheless, a transmission line model taking for input the incident field along the cable $E_{inc}(z)$ will allow the prediction of the voltage and current distribution all along the cable. And the voltage and current distribution along the cable extracted from full-wave simulations were necessary to extract the transmission line parameters which are the impedance per unit length of the cable Z, the admittance per unit length of the cable Y, and the load impedances at both ends

Z_{LOAD_1} and Z_{LOAD_2}. The current distribution $I(z)$ was extracted directly from the current density map. The voltage distribution $V(z)$ was considered to be the integration of the electrical field component perpendicular to the cable in the x-direction until it reaches less than 1% of its maximum value which is at the interface with the perfect electrical conductor. If the cable embedded in gel follows a transmission line model, the distribution of $I(z), V(z)$ and $E\_incident(z)$ should follow the transmission line model equation 1 and 2 associated to the two boundary conditions 3 and 4, z_1 and z_2 being the z coordinate of the ends of the cable. These boundary conditions introduce the simple passive electrode model proposed in this work. Therefore, knowing these distributions allows to extract $Z(z)$ and $Y(z)$ which should be constant if the hypothesis of a transmission line model is right. Z_{LOAD_1} and Z_{LOAD_2} can be extracted as well.

$$\frac{dI}{dz} = -YV \quad [1]$$

$$\frac{dV}{dz} = E_{inc} - ZI \quad [2]$$

$$V(z_1) = -Z_{LOAD_1} I(z_1) \quad [3]$$

$$V(z_2) = Z_{LOAD_2} I(z_2) \quad [4]$$

Parameters extracted from the full-wave simulations were then used in a finite difference model of 1 to 4 to predict voltage and current distributions of the original simulation.

Hertel *et al.* [13] give analytical expression of the parameters Z and Y for simple geometries of insulated antennas. These parameters were compared to those extracted from the full-wave simulation. Associated to the values of the loads extracted from these same simulations, they will be used as an input for the finite difference model to compare the results to the original full-wave distributions.

Different lengths and different termination conditions of the same type of cable were considered to check that the transmission line model has indeed a predictive value for other cables than the one used to extract the model. We considered a 30 cm cable uncapped at both ends as well as a 20 cm cable capped at one end. For the load of the capped cable at the capped end, we used two different values of Z_{LOAD_2} . First 1 MΩ to simulate an open circuit as it is isolated from the gel, second a load extracted from the full-wave simulation as for the first cable studied. The extracted parameters were used at inputs for the transmission line finite difference model for both cables and the results were compared to the full-wave simulations.

From the modified transmission line model to the transfer function model.

Finite difference model

Solving equation (1) to (4) for an incident field Einc with a finite difference method can be written under the following matrix form $\begin{bmatrix} Dz1 & Z \\ Y & Dz2 \end{bmatrix} \begin{bmatrix} V \\ I \end{bmatrix} = \begin{bmatrix} Einc \\ 0 \end{bmatrix}$. The submatrices Dz1, Z, Y and Dz2 have a dimension NxN with N the number of discretization points along the cable. The boundary conditions are implemented at the Nth and last line of the whole matrice. The value that is directly related to

the scattered electric field at the electrode is the voltage at the load modeling the electrode. To solve the finite difference model we inversed the square matrix. The transfer function seen from the left electrode corresponds to the N-1 values of the first line of the inverse matrix, and the transfer function seen from the right electrode corresponds to the N-1 values of the Nth line of the inverse matrix.

Wave propagation model

Another way of considering the problem is to consider that the incident field at a certain position propagates in both ways with a propagation constant k related to the transmission line parameters by $k = \sqrt{-ZY}$ [6] and is reflected at each end with a reflection coefficient ρ that can be calculated by the following classical transmission line equations 5 and 6.

$$Z_C = \sqrt{\frac{Z}{Y}} \quad [5]$$

$$\rho = \frac{Z_{LOAD} - Z_C}{Z_{LOAD} + Z_C} \quad [6]$$

Considering that the origin of the z axis is at the electrode we want the scattered electrical field from, that the reflection coefficient at this end is ρ1 and ρ2 at the distal end and that the length of the isolated part of cable is l, the transfer function at position z can be written:

$$TF(z) = e^{-ikz} - \rho_2 e^{-ik(2l-z)} + \rho_1\rho_2 e^{-ik(2l+z)} - \rho_2\rho_1\rho_2 e^{-ik(4l-z)} \quad [7]$$

$$+\rho_1\rho_2\rho_1\rho_2 e^{-ik(4l+z)} - \rho_2\rho_1\rho_2\rho_1\rho_2 e^{-ik(6l-z)} + \ etc \ \ldots$$

For a 16 cm capped wire of the type SAIMD-1 of the ISO-TS 10974 norm [11] for active implants the value of the transfer function converges with a error of less than 1% if one considers 9 terms and is in accordance with the transfer function derived from the finite difference model described above with an difference of about 7%. In this work, this wave propagation model was considered to be the more reliable because analytic and was used to calculate the transfer functions from the transmission line model.

Validation

Comparison with experimental and simulated transfer functions

The cable tested was the same as the uncapped cable one used in numerical study but with a total length of 53 cm.

Direct comparison

The transmission line model was determined partly from analytical formulas for the impedance and admittance per unit length and Z and Y [13] and from the previous SEMCAD-X simulation for the load impedances. Using the wave propagation model, the transmission line model was used to predict a transfer function.

We have measured the transfer function with a set up based on the reciprocity approach described by Feng et al. [5]. We excited the electrode we wanted to know the power deposited with a simple monopole at and measured the current along the cable. The cable was placed in an ASTM phantom

as described on Figure 1. The transfer function was given by the transmission parameter S21 between the excitation probe and the current probe measured with a vector network analyzer. It was measured every cm.

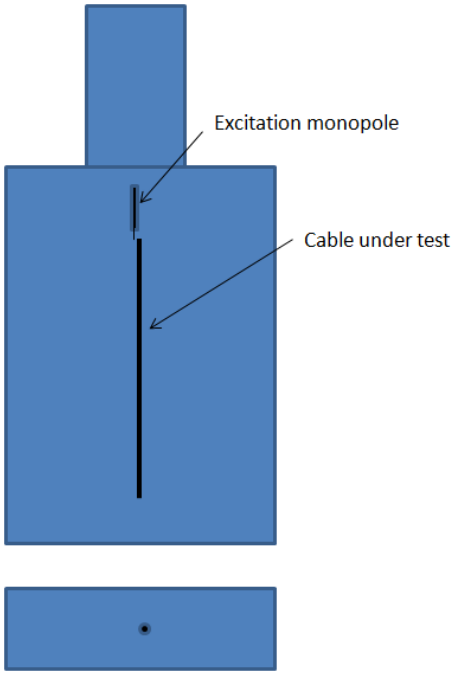

Fig. 1 Setup for the measurement and simulation of the transfer function.

The transfer function predicted by the transmission line model was also compared to a simulated transfer function based on the reciprocity approach. The excitation scheme of the experimental setup was reproduced and the current distribution along the cable directly extracted from the simulation results. The simulation software was CST MICROWAVE STUDIO® (CST® MWS®, Darmstadt, Germany). Nyenhuis *et al.* [14] demonstrate that the measured transfer function with the direct approach depends on the boundaries of the phantom it is measured in. It is also the case for the simulated transfer function based on the reciprocity approach. The transmission line model extracted from the full-wave SEMCAD simulations is a transmission line of the cable in an infinite volume of gel. Therefore the results on the transfer functions are likely to be different.

Solving the inverse problem

As mentioned earlier the transfer function is fully determined by the transmission line propagation constant k and two reflection coefficients through equation 7. The inverse problem was solved for both the experimental and simulated transfer function first letting the two parameters k, and ρ (the reflection coefficient being in our case the same at both ends) free and second by fixing the constant propagation to the value given by the analytical formulas [13] and letting the reflection coefficient free. In the second case the analytical formulas give also the characteristic impedance of the cable therefore from the reflection coefficient one can deduce the load impedance Z_{LOAD}. The parameters k, ρ and Z_{LOAD} extracted to best fit the experimental and simulated transfer functions were compared to the analytical parameters and the full-wave extracted Z_{LOAD}. The inverse problem was also solved using the finite difference model and not the wave propagation model for comparison.

Resonant behaviour of a capped and uncapped cable in an ASTM phantom as a function of cable length.

Cable configurations

The cable type tested was the same as the one used for the transfer function study. Different lengths of the capped cable and uncapped cable were tested. The cables were placed at a position x=130 mm at the right of an ASTM phantom [12] when looking from the bottom of the torso. The phantom was positioned head first in a birdcage and the static 1.5 T field pointed to the head of the phantom. The center of the torso was placed at the isocenter of the MRI bore on the x and z axis and at y=-55 mm, the y axis pointing up. The cable was positioned 45 mm under the surface of gel which was 90 mm deep. The uncapped end of the cable where the temperature was measured was always positioned at the bottom of the torso at z=215mm (the z axis pointing to the bottom of the torso). The heating at the electrode was measured for 14 different lengths ranging from 16 cm to 53 cm for each of the capped and uncapped cables. The set of experiments were conducted twice for the capped cable giving an idea of the uncertainty of the measurement results.

Sequence

The sequence run was the Fast Spin Echo sequence described in the ASTM F2182 norm [12] on a 1.5T GE scanner with the number of slices fixed to 42, the transmit gain to 130 and a nex of 2 which makes a total duration of 6 min 34 s. The mean SAR in the ASTM phantom corresponding to this transmit gain is 1.38 +/-0.11 W/kg according to the calorimetric measurements made following the ASTM heating norm [12].

Full-wave simulation

The exact experiments were reproduced using the full-wave simulator CST MWS. The 1.5T birdcage model used was validated by comparison of the B1 map in the ASTM phantom. The result extracted was the mean loss on a 2 mm cube of gel at the uncapped end.

Transmission Line Model

The same 1.5T birdcage model as for the full-wave simulation was used to simulate the incident field at the position of the cables which was the input to the model. The transmission line model was the one determined from solving the inverse problem on the simulated transfer function fixing k to the analytical values and calculating the best fitting value for the reflection coefficient. The reflection coefficient for the capped end was considered to be one. The wave propagation model with the transmission line parameters will be used to predict the transfer function for each length of cable. The transfer function associated to the simulated incident electrical field allows to predict the scattered electrical field at the electrode. The temperature increase is proportional to the square of the scattered electrical field.

Scaling

A scaling has to be applied corresponding to the calibration procedure for the transfer function [2]. The scaling factor for the full-wave simulation results and the transmission line model results were calculated such that the error with the experimental results was minimized.

RESULTS

Determination of a transmission line model from a full-wave simulation

Figure 2 shows the current and voltage distribution along the uncapped and capped 20 cm cables extracted from the full-wave simulation with a plane-wave excitation. One can notice the asymmetry induced by the different termination conditions at both ends for the capped cable compared to the uncapped one.

Figure 3 shows the norm and phase of $Z(z)$ and $Y(z)$ along the uncapped and capped 20 cm cables extracted using equation 1 and 2. The load impedances model the bare part of the cable for uncapped ends, so the uncapped cable is considered to be situated between -0.09 m and 0.09 m and the capped cable between -0.09m and 0.1m. The results of Figure 3 show that $Z(z)$ as well as $Y(z)$ seem to be approximately constant along the cables therefore demonstrating that the hypothesis of a transmission line behavior of a cable embedded in gel holds. If one looks more precisely, one can notice that $|Z|$ varies quite notably along the length of the cables. The relative difference between the value of $Z(z)$ along the uncapped cable compared to the value at the center reaches 30%. For the admittance per unit length $Y(z)$, ignoring the singularity at the center due to the small voltage values , the relative difference along the cable can reach 20%.

The load impedance of the bare electrode is calculated by using equation 3 and 4 at the positions z=+/- 0.09m. The load impedance for this electrode is found to be 51.3-j 32.7 ohm.

Although the characteristic parameters of the transmission line seem to vary along the uncapped cable, we fixed them to the value at the center for Z and to the mean value of the values at +/-0.05 m for Y. Associated to the value of the load impedance, we used them as an input to the finite difference transmission line model. Table 1 sums up the results on the error on the voltage and current distribution for the full-wave simulation extracted model (Model 1) and the one using analytical formulas for *Z* and *Y* [13] associated to Z_{LOAD} from the simulation (Model 2).

	Z	Y	ZLOAD	Error I	Error V
Model 1 (full_wave)	91.5+j 324.6	0.0071+j 0.0972	51.3-j 32.7	3.17%	2.97%
Model 2 (analytical, Z_{LOAD} full-wave)	85.1+j 361.8	0.0073+j 0.0939	51.3-j 32.7	6.02%	7.56%

Table 1 Error of the transmission line models with constant parameters on the full-wave current and voltage distribution for a 20 cm uncapped cable.

One can notice that the fact of fixing the characteristic parameters to a certain constant value allows to predict the current and voltage distribution of the full-wave simulation with an error of less than 5%. The parameters extracted from the simulation are close to the parameters given by the analytical formulas [13], and these allow to retrieve the full-wave distributions with a relative quadratic error of less than 10%.

Figure 3 also shows the amplitude and phase of $Z(z)$ and $Y(z)$ for a 20 cm capped cable to be compared to the uncapped case. The results are in accordance. The differences can be attributed to numerical errors.

The load impedance at the capped end extracted from the full-wave simulation was 2203 –j 1969 ohm. Considering that the capped end corresponds to an infinite impedance means that the

reflection coefficient is 1. With the full-wave simulation load impedance and the analytical transmission line parameters the reflection coefficient is found to be 0.965-j0.026.

The results concerning the ability of the transmission line model determined from the simulation on the 20 cm uncapped cable to retrieve the current and voltage distribution of the full-wave simulation for a 30 cm uncapped cable and a 20 cm capped cable are summarized in Table 2.

	20 cm capped cable		30 cm uncapped cable	
	Error I	Error V	Error I	Error V
Model 1(full-wave)	8.34%	3.64%	3.04%	5.2%
Model 2 (analytical, full-wave)	6.82%	3.37%	7.99%	5.3%
Model 1 (full-wave/ infinite load 1 MΩ)	12.65%	3.29%	x	x
Model 2 (analytical/ infinite load 1 MΩ)	11.4%	4.69%	x	x

Table 2 Error on the voltage and current distribution of a 20 cm capped and 30 cm uncapped cables of the transmission line model with constant parameters extracted from full-wave simulation on a 20 cm uncapped cable. The reference distributions are from full-wave simulations.

For both the 20 cm capped and 30 cm uncapped cable, the full-wave extracted model and the mixed analytical/ full-wave model predict the current and voltage distribution of the full-wave simulation with an error on the distribution of less than 10%. Fixing the reflection coefficient of the capped end to 1 makes the error on the current distribution increase to slightly above 10%, the voltage error remaining under 5%. The mixed analytical/full-wave model gives results as good as the full-wave extracted model.

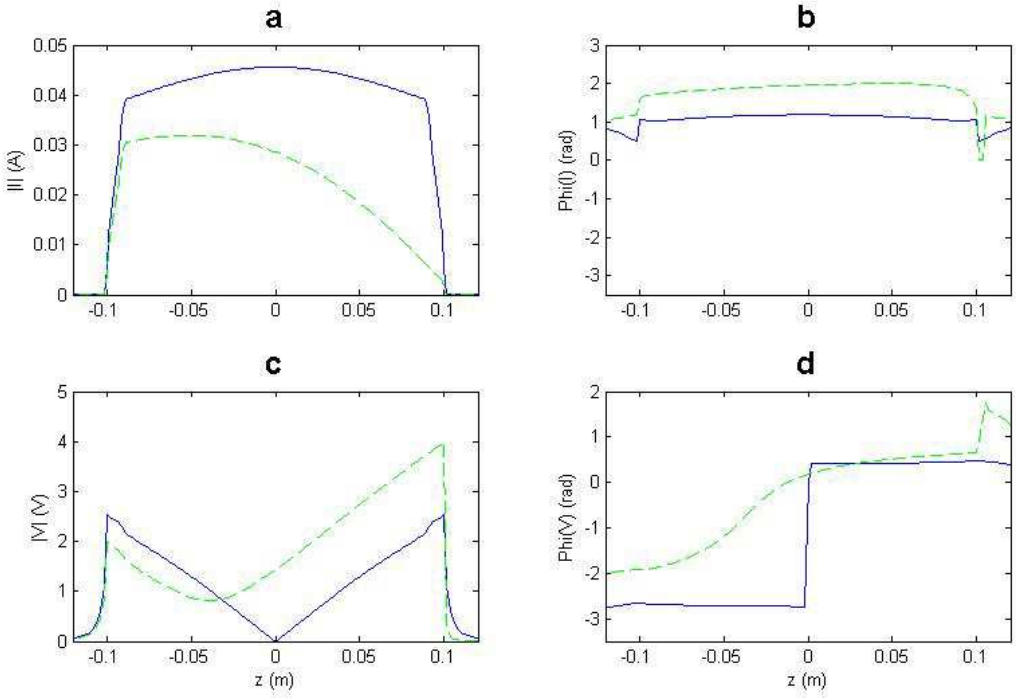

Fig. 2 Distribution of amplitude and phase of current and voltage for an uncapped 20 cm cable (solid blue line) and a capped 20 cm cable (dashed green line). The capped end is at +0.1m. a) amplitude of current, b) phase of current, c)amplitude of voltage, d) phase of voltage.

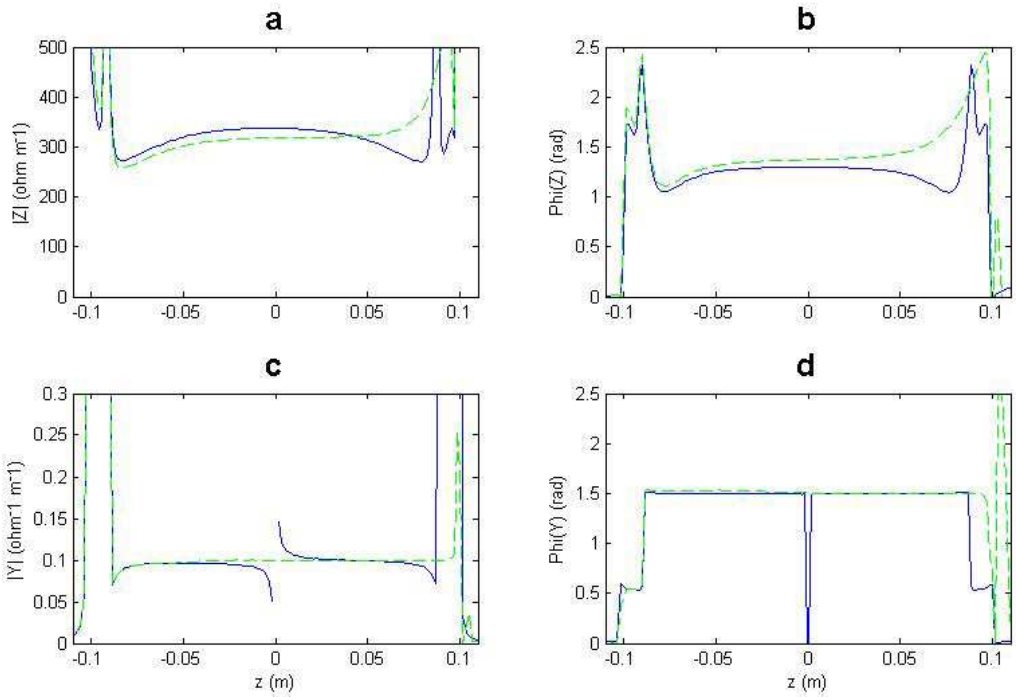

Fig. 3 Amplitude and phase of the impedance per unit length Z and admittance per unit length Y as a function of position along the cable if one makes the transmission line model assumption. The blue solid line represents the results for an 20 cm uncapped cable, the green dashed line represent the results for a 20 cm capped cable isolated at the position +0.1m.a) amplitude of impedance per unit length, b) phase of impedance per unit length, c) amplitude of admittance per unit length, d) phase of admittance per unit length.

Validation

Comparison with experimental and simulated transfer functions

Direct comparison

Figure 4 shows the experimental and full-wave simulated transfer function. The green line shows for comparison, the transfer function predicted by the transmission line model with the analytical propagation constant and the full-wave load impedance. The phase distribution fits nearly perfectly. The amplitude distribution has the same global trend but one can observe a shift of the local maximum and minimum towards the distal end.

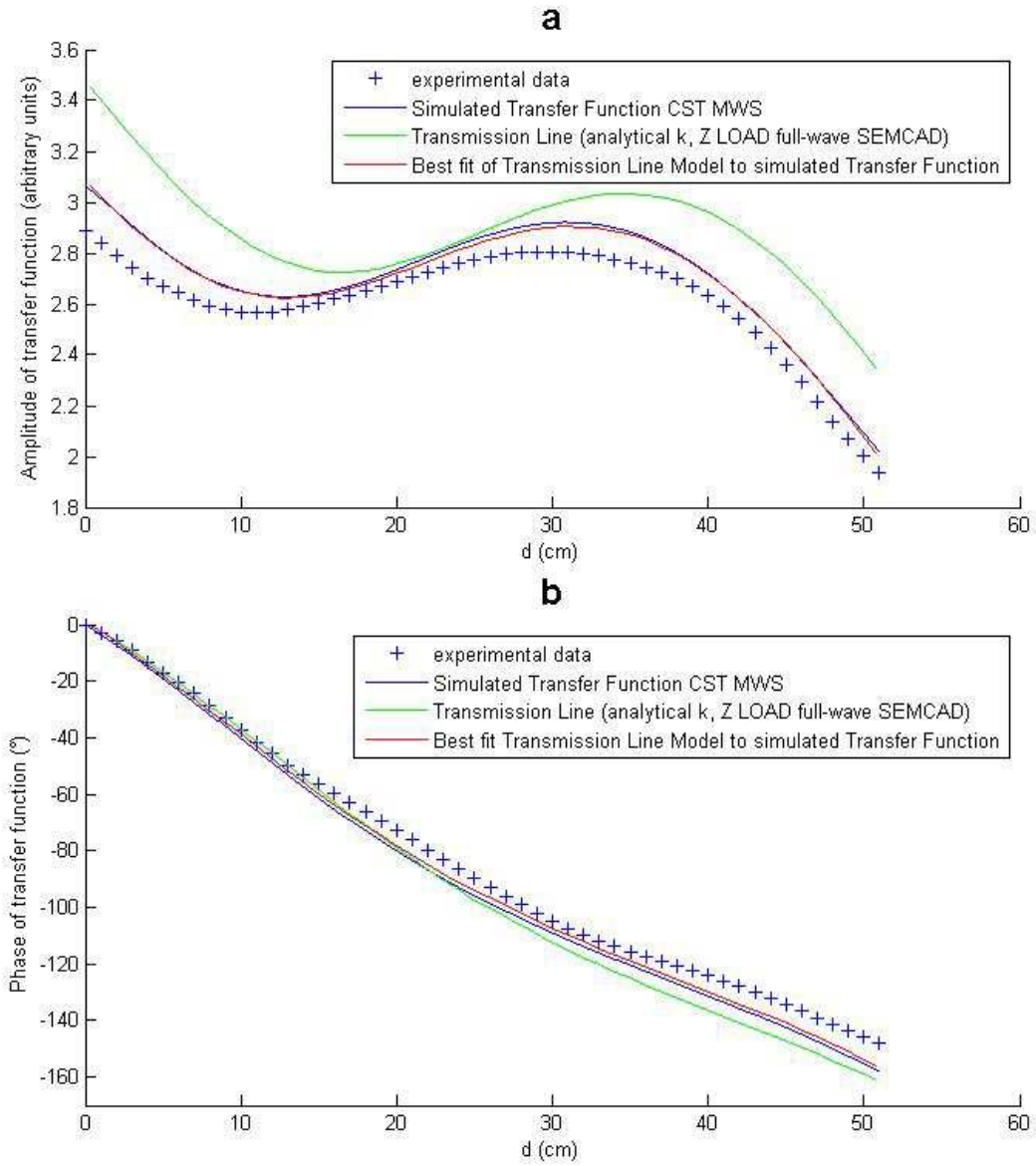

Fig. 4 Experimental and different models amplitude and phase distribution of the transfer function of a 53 cm uncapped cable. a) Transfer function normalized amplitude, b) Transfer function Phase. The electrode the heating will be evaluated at is at position d=0 cm

Solving the inverse problem

The red line of Figure 4 corresponds to the transmission line model extracted by best fitting the simulated transfer function according to equation 7 using the analytical propagation constant. Table 3 shows that the transfer function perfectly fits a transmission line model but with a load impedance slightly different from the one determined from the full-wave simulation.

Table 3 also sums up the results on the propagation constant k, the reflection coefficient ρ and the load impedance Z_{LOAD} of solving the inverse problem from the experimental and simulated transfer functions. The fit leaving the propagation constant k free gives a result very close to the analytical propagation constant for the simulated transfer function and slightly different for the experimental transfer function. The finite difference model also allows to solve the inverse problem and gives results comparable to the wave propagation model.

	k	ρ	Z_{LOAD}	Error of fit
Analytical (k) + full-wave (ZLOAD)	5.84-j0.90	-0.02-j0.25	51.3-j32.7	x
Inverse k, ρ on experimental TF data	5.49-j0.91	0.04-j0.25	x	2.7%
Inverse k, ρ on simulated TF data	5.75-j0.90	0.07-j0.25	x	0.6%
Inverse ρ (ZLOAD) on experimental TF data, k analytical	x	0.17-j0.19	79.2-j38.7	7.8%
Inverse ρ (Z_{LOAD}) on simulated TF data, k analytical	x	0.11-j0.24	66.1-j39.9	2.1%
Inverse ρ (Z_{LOAD}) on simulated TF data, k analytical (Finite Difference Model)	x	0.04-j0.25	65.2-j40.6	1.8%

Table 3 Results on the propagation constant k, the reflection coefficient of the uncapped end ρ, and the load impedance of the uncapped end solving the inverse problem of getting these parameters from the simulated and experimental transfer function of an uncapped 53 cm cable

Resonant behaviour of a capped and uncapped cable in an ASTM phantom as a function of cable length.

Figure 5 shows the resonant behavior of the capped and uncapped cable placed in an ASTM phantom in a 1.5T birdcage as a function of length. The full-wave simulation results (green line) coincide well with the results predicted by the transmission line model extracted from the simulated transfer function (black line). There is a shift of a few cm of the resonant length. The trend of the experimental data is the same as the trend of the full-wave model and the two different transmission line extracted model. There is a high uncertainty of the temperature increase measurement for higher temperature. This is due to the fact that for higher temperature increases the temperature gradients around the electrode are higher inducing a greater sensitivity of the measurement on the temperature probe position.

The results on the resonant behavior of the uncapped are also consistent. Especially the shift of the resonant length between the capped and uncapped cable is correctly predicted by the different models. The sharper increase of the temperature elevation with the length for the capped cable compared to the uncapped cable is also correctly predicted.

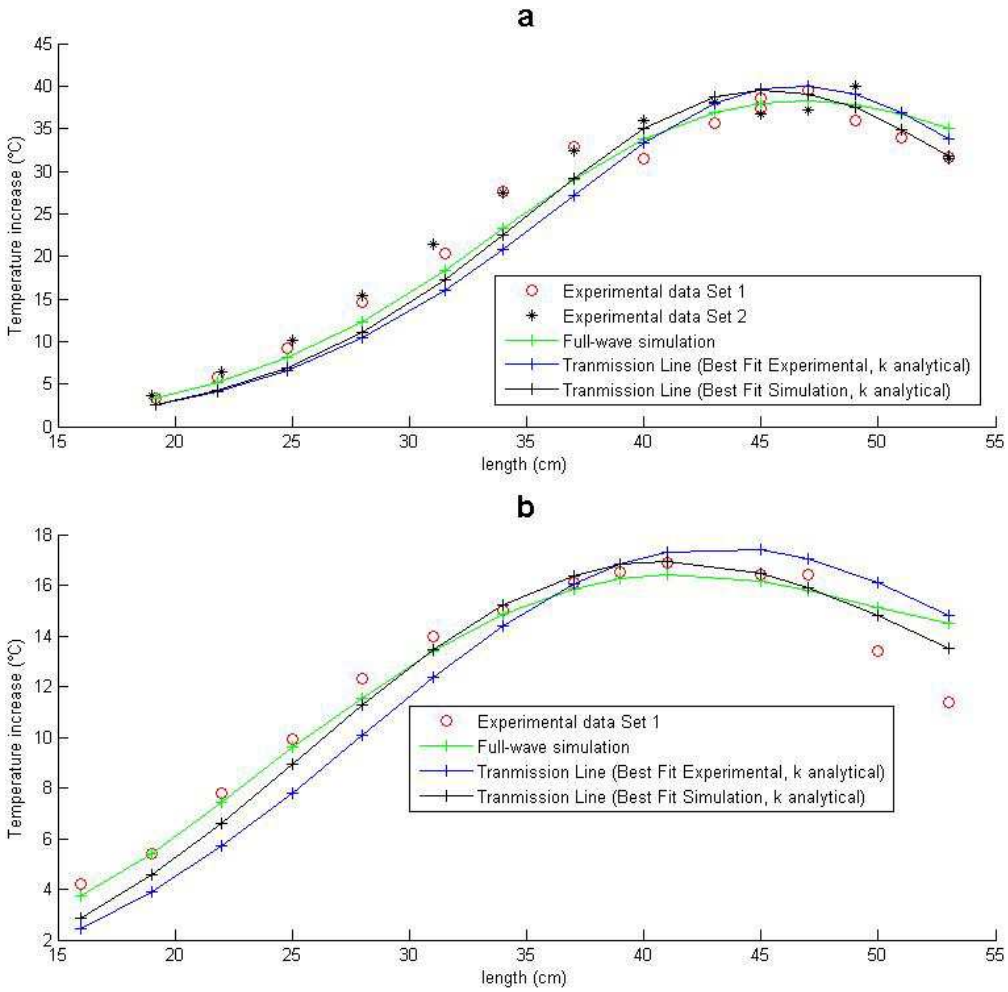

Fig. 5 Temperature increase at the uncapped end of capped and uncapped cable placed in an ASTM phantom in a 1.5T MRI as a function of length of the cable. The prediction of the transmission line models best fitting the simulated and experimental transfer function are compared to experimental data. a) capped cable, b) uncapped cable.

The full-wave simulation results slightly differ from the results predicted by the transmission line model extracted by solving the inverse problem on the simulated transfer function. One has to recall that the simulate transfer function depends on the position of the cable inside the phantom. The full-wave simulations were made with the cable placed in the position it was in the experiments which is different from the position used for the transfer function simulation. This probably explains the difference in the predicted temperature elevation as a function of the length of the cable.

DISCUSSION

Full-wave simulations

It has been shown using full-wave simulations of an insulated cable embedded in gel that the current and voltage distribution along the cable do follow approximately a transmission line behavior. Supposing it strictly follows a transmission line behavior still gives results consistent with the full-wave simulation.

From a transfer function model to a transmission line model

It was shown that simulated and experimental transfer function can fit nearly perfectly a transmission line model showing the underlying assumption under the transfer function model is indeed a transmission line model [2, 5]. Therefore the behavior of a simple cable submitted to the radiofrequency field of a 1.5T MRI can be entirely described by a physical set of parameters instead of a mathematical transfer function model. Especially as the termination conditions play a crucial role [15], it can link the heating at the bare electrode to the reflection coefficient at the distal end. More generally, this can help in the design of safe cables as this model enables to link directly the geometrical and physical properties of the cable to the heating risk in MRI for any incident field. For example, it was possible to predict the experimental resonant behavior as a function of length of a capped and uncapped cable from the simple set of very few parameters without having to evaluate experimentally or with full-wave simulations the transfer function for each length.

Load impedance model

This work combined the work by Acikel *et al.* [7] which extended the work by King[4, 6] for a cable excited by a field distribution with the simple model of the bare electrode proposed by King [4, 8]. Instead of being calculated analytically considering it as a monopole as in [8], the load model was first extracted from full-wave simulation data then determined from solving the inverse problem from transfer function data. The results showed that the load was not exactly the same. The most relevant method in the future seems to be to get the load or reflection coefficient from the experimental or simulated transfer function. Indeed the high field distribution around the bare electrode will be very sensitive to numerical errors. Further work would be to compare for simple cables, the load model determined from the transfer function and the analytical value from King [8].

Transmission line model for pacemaker leads

One has to remind oneself that the transfer function concept was thought mainly for cables one cannot simulate. Therefore it is important to be able to get the information from experimental data for example, an experimentally measured transfer function. There are nevertheless two problems arising for leads of typical medical devices such as pacemakers. If someone wants to reduce the heating at the electrode by varying the reflection coefficient at the distal end meaning at the case, it is necessary in the future to develop tools to directly evaluate this coefficient either theoretically or experimentally without measuring the new transfer function each time. Nevertheless, the transmission line will still give a better physical insight of the behavior of the pacemaker lead in the radiofrequency field. A second problem arising comes from the fact that pacemaker leads are usually made of two coaxial helicoidal wires. The transmission line model developed here was for cables made of one wire only. Further work needs to be carried on to see if it is possible to consider a coupled transmission line model for cables made of multiple wires which will be a model with supplementary coupling parameters such as a distributed mutual inductance and a distributed mutual capacitance.

CONCLUSION

A new transmission line model was developed for simple cables made of one wire submitted to a radiofrequency excitation field at 64 MHz and embedded in tissue properties imitating gel. The

termination conditions were modeled by a simple passive load impedance that has a physical meaning. It was shown that it has a strict equivalence with the transfer function model and it brings physical insight into it. This physical insight can help in the design of safe cables in MRI.

REFERENCES

1. Talcoth O, Rylander T (2011) Electromagnetic Modeling of Pacemaker Lead Heating during MRI.

2. Park S-M, Kamondetdacha R, Nyenhuis JA (2007) Calculation of MRI-induced heating of an implanted medical lead wire with an electric field transfer function. J. Magn. Reson. Imaging 26:1278–1285.

3. Yeung CJ, Susil RC, Atalar E (2002) RF heating due to conductive wires during MRI depends on the phase distribution of the transmit field. Magn. Reson. Med. 48:1096–1098.

4. King R (1986) Antennas in material media near boundaries with application to communication and geophysical exploration, Part II: The terminated insulated antenna. IEEE Trans. Antennas Propag. 34:490–496.

5. Feng S, Qiang R, Kainz W, Chen J (2015) A Technique to Evaluate MRI-Induced Electric Fields at the Ends of Practical Implanted Lead. IEEE Trans. Microw. Theory Tech. 63:305–313.

6. King RWP (1976) The many faces of the insulated antenna. Proc. IEEE 64:228–238.

7. Acikel V, Atalar E (2011) Modeling of radio-frequency induced currents on lead wires during MR imaging using a modified transmission line method. Med. Phys. 38:6623–6632.

8. King RWP, Sandler B, Wu TT (1969) Cylindrical Antennas Immersed in Arbitrary Homogeneous Isotropic Media. J. Appl. Phys. 40:5049–5065.

9. Acikel V, Uslubas A, Atalar E (2015) Modeling of electrodes and implantable pulse generator cases for the analysis of implant tip heating under MR imaging. Med. Phys. 42:3922–3931.

10. Acikel V, Atalar E Determining RF Safety Conditions of Implant Leads Using MoTLiM. In: Proc. Intl. Soc. Mag. Reson. Med 2014. Milan, Italy, 2014.

11. ISO/TS 10974 (2012), Assessment of the safety of magnetic resonance imaging for patients with an active implantable medical device. International Organization for Standardization, Geneva, Switzerland, http://www.iso.org/iso/catalogue_detail.htm?csnumber=46462. 20 May 2013

12. ASTM F 2182A (2011) Standard Test Method for Measurement of Radio Frequency Induced Heating On or Near Passive Implants During Magnetic Resonance Imaging. http://www.astm.org/Standards/F2182.htm

13. Hertel TW, Smith GS (2000) The insulated linear antenna-revisited. IEEE Trans. Antennas Propag. 48:914–920.

14. Nyenhuis J, Jallal J, Min X, Sison S, Mouchawar G Comparison of measurement and calculation of the electric field transfer function for an active implant lead in different media. In: 2015 Computing in Cardiology Conference (CinC)., 2015:765–768.

15. Langman DA, Goldberg IB, Finn JP, Ennis DB (2011) Pacemaker lead tip heating in abandoned and pacemaker-attached leads at 1.5 tesla MRI. J. Magn. Reson. Imaging 33:426–431.